Life Sciences 233 (2019) 116741

Contents lists available at ScienceDirect

Life Sciences

journal homepage: www.elsevier.com/locate/lifescie

Lysosomal dysfunction is associated with persistent lung injury in dams caused by pregnancy exposure to carbon black nanoparticles

Xuemei Liu[a,1], Baijie Tu[a,1], Xuejun Jiang[b], Ge Xu[c], Lulu Bai[a], Longbin Zhang[a], Pan Meng[a], Xia Qin[d], Chengzhi Chen[a,e,*], Zhen Zou[c,e,**]

[a] Department of Occupational and Environmental Health, School of Public Health and Management, Chongqing Medical University, Chongqing 400016, PR China
[b] Center of Experimental Teaching for Public Health, Experimental Teaching and Management Center, Chongqing Medical University, Chongqing 400016, PR China
[c] Institute of Life Sciences, Chongqing Medical University, Chongqing 400016, PR China
[d] Department of Pharmacy, The First Affiliated Hospital of Chongqing Medical University, Chongqing 400016, PR China
[e] Dongsheng Lung-Brain Disease Joint Lab, Chongqing Medical University, Chongqing 400016, PR China

ARTICLE INFO

Keywords:
Pregnancy exposure
Carbon black nanoparticles
Persistent lung injury
Lysosomal dysfunction

ABSTRACT

Aims: Carbon black nanoparticles (CBNPs) are widely used in industrial field. Sensitive stages such as pregnancy are assumed to be more susceptible to stimulus, however whether pregnancy exposure to CBNPs (PrE-to-CBNPs) would cause long-term toxic effects in dams and the underlying mechanisms remain poorly addressed. The present study is aimed to determine the long-term toxic effects of PrE-to-CBNPs in dams.

Materials and methods: The pregnant mice were randomly divided into control group, low (21 μg/animal), medium (103 μg/animal) and high (515 μg/animal) CBNPs-treated groups. From gestational day (GD) 9 to GD18, the pregnant mice were intranasal exposed. At 49 days after parturition, lung tissues and bronchoalveolar lavage fluid (BALF) were obtained. Weight change, lung histopathology, lung ultrastructural pathology, cell count in BALF, oxidative stress/inflammatory maker and autophagy/lysosome-related protein expression were determined.

Key findings: PrE-to-CBNPs caused a dose-dependent persistent lung injury in mice even 49 days after parturition, including the deteriorative lung histopathological changes, elevation of oxidative stress marker Nrf-2, HO-1 and CHOP, infiltration of macrophage and increased mRNA expression of inflammatory cytokines in the lung tissues and elevation of cells in BALF. However, PrE-to-CBNPs did not induce significant neutrophil infiltration and fibrosis. Moreover, we found that CBNPs could deposit in the lysosomes and decrease cathepsin D (an important hydrolase in lysosome), which might be associated with the dysfunction of lysosome and autophagy.

Significance: Our study demonstrated that PrE-to-CBNPs could result in long-term lung injury in dams, and lysosomal dysfunction was probably linked to this process.

1. Introduction

Carbon black nanoparticles (hereafter referred as CBNPs) are widely used in rubber, paints and inks etc. [1]. With large specific surface area, CBNPs can display toxic profiles that are very different from its coarse particles [2]. The toxic effects of CBNPs have been investigated in recent years, and CBNPs exposure have been linked to a number of biologic pathologies, including inflammation, fibrosis, and genotoxicity [3–8]. Previous studies primarily focused on the toxic effects induced by CBNPs in adult mice. Recently, there is an increasing concern that exposure to CBNPs during sensitive stages, such as fetal life or early postnatal period, may produce unpredictable harmful effects in both dams and offspring because of altered hormone level and unmatured immune system. Indeed, the adverse effects have been reported in pregnant animals and their pups after intratracheal instilled with CBNPs during pregnancy [9,10]. Even so, scarce studies addressed whether long-term toxic effects would be caused by pregnancy exposure to CBNPs in dams. In our recent study, we found that pregnancy exposure to CBNPs induced brain pathological changes and cerebrovascular dysfunction in female mice [11]. Given that lung is the

* Corresponding author at: Department of Occupational and Environmental Health, School of Public Health and Management, Chongqing Medical University, Chongqing 400016, PR China.
** Correspondence to: Z. Zou, Institute of Life Sciences, Chongqing Medical University, Chongqing 400016, PR China.
E-mail addresses: chengzhichen@cqmu.edu.cn (C. Chen), zouzhen@cqmu.edu.cn (Z. Zou).
[1] These two authors contributed equally to this work.

https://doi.org/10.1016/j.lfs.2019.116741
Received 17 June 2019; Received in revised form 31 July 2019; Accepted 6 August 2019
Available online 06 August 2019

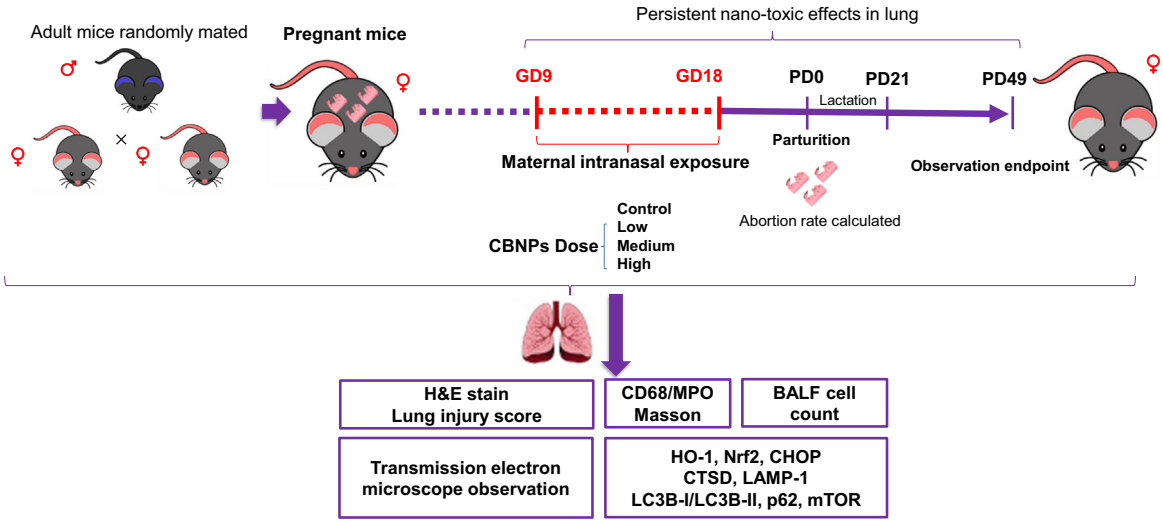

Fig. 1. Scheme of this study.
Notes: For the details, referring to the study design described in the Animal and study design section.

primary target organ of CBNPs exposure, we suspect that long-term lung injury in dams also occurred after CBNPs pregnancy exposure.

Autophagy is an intracellular degradation system that delivers cytoplasmic constituents (*e.g.*, aberrant protein/mitochondria) to the lysosomes. Lysosomes are the degradative organelles of the cell and contain an acidic lumen to allow specialized hydrolases to break down protein, lipid, carbohydrate and nucleic acids. As lysosomes are the final destination, inhibition of lysosomal function will disrupt autophagic pathways, which is termed as impaired autophagic flux [12,13]. Autophagy is commonly recognized as a cytoprotective mechanism through which cells maintain homeostatic functions, whereas impaired autophagic flux is linked to uncontrolled reactive oxygen species (ROS) production and inflammation [14–16]. Recently, autophagic and lysosomal dysfunction have been recognized as emerging mechanisms for nanomaterials-induced toxicity [17], however whether autophagic and lysosomal dysfunction are involved in long-term lung injury induced by PrE-to-CBNPs in dams is not addressed.

Herein, we provided the first evidence that pregnancy exposure to CBNPs could result in sustained lung injury even after 49 days after parturition in dams, including induction of oxidative stress and inflammation. Interestingly, lysosomal dysfunction was probably associated with this process.

2. Materials and methods

2.1. Chemicals and reagents

Hematoxylin-Eosin stain kit and masson stain kit were obtained from Nanjing Jiancheng Institute of Bioengineering (Jiangsu, China); immunohistochemistry assay kit was purchased from Zhongshan Golden Bridge Biotechnology Co., Ltd. (ZsBio, Beijing, China); antibodies against LC3B (L7543) and p62 (P0067) were obtained from Sigma-Aldrich (MO, USA); antibodies against HO-1 (ab68477), p-mTOR (Ser2448) (ab109268) and anti-myeloperoxidase antibody [EPR20257] (ab106568) were obtained from Abcam (Cambridge, UK); antibodies against CTSD (sc-377299) and LAMP-1 (sc-19992) were purchased from Santa Cruz (CA, USA); anti-CHOP (15204-1-AP), anti-Nrf-2 (16396-1-AP) and anti-CD68 (28058-1-AP) antibody were purchased from Proteintech (Wuhan, China); anti-GAPDH antibody (bs-10900R) and anti-β-actin antibody (bs-0061R) were obtained from Bioss Biological Technology Co. Ltd. (Beijing, China).

2.2. Animals and study design

Healthy specific pathogen free female and male C57BL/6J mice, aged 8 weeks and weighed 22–25 g, were obtained from Experimental Animal Center of Chongqing Medical University [Chongqing, China, license numbers: SCXK(Yu)2012-001]. The current study was approved by the Institutional Animal Care and Use Committee of Chongqing Medical University.

The mice were kept in controlled environment with temperature 23 ± 1 °C, humidity 55 ± 10% and 12-h light/12-h dark cycle. After the 7-day acclimatization, the nulliparous female mice were mated with males (2:1) at 6:00 PM. On the next morning, mating was confirmed by the observation of a copulatory plug in vaginal-cervical region. Once mating was confirmed, the pregnant mice were randomly assigned to control group, low (21 μg/animal), medium (103 μg/animal) and high (515 μg/animal) CBNPs-treated groups and housed individually in cages. The day of presence of copulatory plug was recorded as gestational day 1 (GD1). From GD 9 to GD18, the pregnant mice were intranasally administrated with either CBNPs suspension or ultrapure sterile water once a day at 2:00 PM and 3:00 PM. Intranasal exposure by placing a pipette tip with the dosing solution (20 μl) into the nostril of the mouse after slightly anesthesia with pentobarbital sodium. After CBNPs exposure, the mice did not show any severe sign of physical symptoms, such as lethargy, respiratory distress or poor feeding. The pregnant mice were treated in different orders each day to reduce any variation that might be related to the time of exposure. After the last CBNPs exposure on GD 18, the pregnant mice were allowed to deliver naturally and were monitored every day. After parturition, the offspring were then counted and sex was determined. The animals were gently sacrificed by cervical dislocation under pentobarbital sodium anesthesia at 49 days post parturition. After verifying the death of mice, the fresh lung tissues were isolated and collected for the designed experiments. The study design was shown in Fig. 1.

2.3. Characterization of CBNPs and preparation

The CBNPs (Printex 90) were obtained from Degussa-Hüls Co. (Frankfurt, Germany). Characterizations of CBNPs have been showed in detail by previous studies [18,19]. Given that the recommended doses for developmental toxicity of CBNPs are not readily available, the doses used in this study was based upon the expected pulmonary dose from the previous Printex 90 studies as well as the Chinese occupational exposure limit of CB. For details, the current 8 hour time weighted

average for the occupational exposure limit (Permissible concentration-time weighted average, PC-TWA) to CB in China is 4 mg/m^3. Therefore, the highest dose (103 μg/animal) in this study corresponds to days of exposure by the Chinese occupational limit. We assumed a worker handled CBNPs for 8 h a day, five working days per week, for a total of 40 h during working week. The average healthy adult inhales and exhales about 10 l of air per minute at rest, and the total inhaled volume of air of a worker was near 24 m^3 (10 L/min × 60 min/h × 40 h). The worker may theoretically inhale about 96 mg CBNPs. In fact, near 90% volume of air will be exhaled during normal breathing. Thus, the actual inhaled dose of worker to CBNPs is 9.6 mg (24 m^3 × 4 mg/m^3 × 10%). Generally, uncertain factor is initially set at 100, with interspecies variation (×10, difference between animal and humans). We can further calculate the doses as the following formula: 9.6 mg × 25 g (presumed mouse weight) × 100 (uncertain factor) ÷ 60,000 (presumed healthy worker body weight) = 400 μg. Therefore, the exposure high, medium and low doses of CBNPs were chosen as 515, 103 and 21 μg/animal. Moreover, in the previous study, Jackson et al., has also revealed that mice were exposed to 42 mg/m^3 of CBNPs for 1 h/day on GD8–18 by a whole-body inhalation exposure system resulting in a total inhaled mass of 826 μg/animal [20], which is similar with our study.

CBNPs Printex 90 were prepared freshly each time and sonicated with an ultrasonic cleaner set at 20% of the maximum amplitude with 10 s pulses were alternated with 10 s pauses (SB-5200DT; Ningbo Scientz Biotechnology Co., Ltd., China) for a total sonication time of 20 min in an ice water bath to ensure their homogeneity. The high concentrations of CBNPs (25.75 μg/μL) were firstly diluted in sterilized ultrapure water. After sonicating, the high dose of CBNPs was further diluted 5 times for the medium dose (5.15 μg/μL) by sterilized ultrapure water, and followed by the same step to make the low dose of CBNPs (1.05 μg/μL).

2.4. Lung edema assessment

The fresh lung tissues were isolated and collected into the pre-weighed centrifuge tubes. The wet weights of lung tissues were measured and recorded. The dry weights of lung tissues were obtained after drying in the oven at 65 °C for 48 h. Ratio of wet-to-dry weight was calculated as the wet lung mass divided by the dry lung mass.

2.5. Measurement of cell count in bronchoalveolar lavage fluid

After exposing and cannulating the upper part of the trachea, the bronchoalveolar lavage fluid (BALF) was collected by lavaging the lung with normal saline as previously described [21]. The BALF were then immediately subjected to centrifuge at 3000 rpm for 10 min at 4 °C. The cell precipitation of BALF was suspended in 1 mL phosphate buffered saline. The total cells in BALF were counted by TC20™ Automated Cell Counter (Bio-Rad, USA).

2.6. Hematoxylin-eosin (H&E) staining

H&E staining was conducted to observe the morphological changes of lung tissues according to the protocols described previously [21]. Briefly, after prefixed in the 4% paraformaldehyde, the sections were prepared by standard pathological procedures. The slides were deparaffinized and dehydrated with gradient ethanol. Next, the sections were stained with hematoxylin for 5 min at room temperature and differentiated with 0.1% hydrochloric acid in 50% ethanol. After washing with running tap water, the slides were stained with eosin for another 5 min. The slides were dehydrated with ethanol followed by clear in xylene and mounted with neutral gum. Lung injury was scored according to lung injury scores as described previously [22].

2.7. Masson's trichrome staining

Collagen fibers in the lung tissues were detected by using Masson's trichrome staining described previously [23]. Briefly, after deparaffinizing and rehydrating with gradient ethanol, the slides were stained in Weigert's iron hematoxylin working solution for 10 min, and rinsed in running warm tap water. The slides were then stained with Biebrich scarlet-acid fuchsin solution for 10 min, and differentiated by phosphomolybdic-phosphotungstic acid solution until collagen is not red. Subsequently, the slides were stained with aniline blue solution for 10 min. After washing by distilled water and differentiating in 1% acetic acid solution, the slides were dehydrate with ethanol, clear in xylene, and mounted by neutral gum.

2.8. Immunohistochemistry

The expressions of CD68 and MPO were determined by immunohistochemistry according to the procedures described previously [21]. In brief, the paraffin-embedded tissues were mounted onto microscope slides. Subsequently, the slides were dehydrated by ethanol and performed antigen retrieval with sodium citrate solution. The slices were then incubated with 3% H_2O_2 to suppress endogenous peroxidase activity at room temperature. After blocking in the goat serum, the slides were incubated with primary antibodies (rabbit CD68 1:100 and anti-MPO, 1:100) at 4 °C overnight. Next day, the slides were incubated with the biotinylated secondary antibody and horseradish peroxidase conjugated streptavidin at room temperature for 20 min, respectively. The slides were then developed in 3, 3′-diaminobenzidine (DAB), dehydrated with ethanol, clear by xylene, mounted with neutral gum. The expressions of target proteins were observed under a microscope (Olympus IX53, Tokyo, Japan).

2.9. Transmission electron microscopy

The procedures of transmission electron microscopy were performed as described previously [21]. In brief, by using the heart perfusion-fixed technique, the lung tissues were fixed with 4% paraformaldehyde and 2.5% (w/v) glutaraldehyde buffer. The tissues were quickly excised and cut into 1 mm^3 in size and fixed in glutaraldehyde and 1.0% osmic acid. The sections were then dehydrated with the gradient ethanol and embedded in epon 812. The tissues were placed on the slide coated with celloidin. Ultrathin sections were then stained with uranyl acetate and lead citrate. Finally, the sections were observed under the transmission electron microscope (Hitachi-7500, Hitachi, Ltd., Tokyo, Japan).

2.10. Western blot analysis

Western blot analysis was used to detect the protein expression as described previously [24]. In brief, the lung tissues were prepared using RIPA lysis buffer supplemented with protease inhibitors cocktail and PMSF. The protein samples were then subject to sodium dodecyl sulfate polyacrylamide gel electrophoresis and electro-blotted onto polyvinylidene fluoride membranes. After blocking with 5% non-fat milk, the membranes were incubated with primary antibodies against anti-LAMP-1 (1:500), anti-HO-1 (1:2000), anti-CTSD (1:600), anti-LC3B (1:2000), anti-p62 (1:3000), anti-p-mTOR (1:2000), anti-Nrf-2 (1:1000), anti-CHOP (1:600), anti-GAPDH (1:5000) and anti-β-actin (1:4000) overnight at 4 °C. Next day, the membranes were incubated with secondary antibodies conjugated with horseradish peroxidase (1:20,000) for 1 h at room temperature. The enhanced chemiluminescence reagents were used to visualize the target proteins by Molecular Imager Gel Doc XR System (Bio-Rad, USA). The protein bands were quantified using Image J software (Bethesda, MA, USA), and the expression of β-actin or GAPDH were served as loading controls.

2.11. Quantitative PCR assay

Total RNA was extracted from lung tissues using Eastep Super Total RNA Extraction Kit (Promega, Madison, WI, USA) according to the manufacturer's instruction. cDNA was synthesized from 1.5 μg of total RNA with Go Script Reverse Transcription Kit (Promega). PCR amplification assays were performed with Go Taq Real-time Quantitative PCR Master Mix (Promega) on CFX Connect Real-Time PCR Detection System (Bio-Rad, CA, USA). The specific primers were synthesized by Sangon Biotech (Shanghai, China) and the sequences were as follow:

Mouse IL-6 forward primer: 5′-CATCCAGTTGCCTTCTTG-3′,
Mouse IL-6 reverse primer: 5′-ATTAAGCCTCCGACTTGT-3′;
Mouse TNF-α forward primer: 5′-TCTCAGCCTCTTCTCATTC-3′,
Mouse TNF-α reverse primer: 5′-GCCATTTGGGAACTTCTC-3′;
Mouse IL-1β forward primer: 5′-GGACAGAATATCAACCAACAA-3′,
Mouse IL-1β reverse primer: 5′-TTACACAGGACAGGTATAGATT-3′;
Mouse β-actin forward primer: 5′-AGCCATGTACGTAGCCATCC-3′,
Mouse β-actin reverse primer: 5′-GCTGTGGTGGTGAAGCTGTA-3′.

The initial denaturation was carried out at 95 °C for 3 min, followed by amplification in 40 cycles of 95 °C for 10 s and 30 s at 55 °C for annealing, using the CFX Connect™ Real-Time System (Bio-Rad).

2.12. Statistical analysis

All experimental data were showed as mean ± S.D. Statistical analysis was performed by Statistical Program for Social Sciences (SPSS) software version 22.0 (IBM Corporation, Armonk, NY, USA). One-way analysis of variance (ANOVA) followed by the *post hoc* Tukey's test was used to compare the significant differences among groups. Kruskal-Wallis test was applied when the data in case of heterogeneity of variance. The significance level was set at *0.05* for all parameters.

3. Results

3.1. Pregnancy exposure to CBNPs resulted in body weight loss

The body weight of pregnant mice of Control, CBNPs-Low, CBNPs-Medium and CBNPs-High groups were recorded. We found that PrE-to-CBNPs caused more pronounced body weight loss compared with Control group from 4 to 6 weeks after parturition (Fig. 2), suggesting that PrE-to-CBNPs might cause long-term toxic effects in mice.

3.2. Pregnancy exposure to CBNPs caused persistent lung injury

Since CBNPs were exposed through nasal instillation, and CBNPs were supposed to be deposited in lung tissue. The results of H&E-stained lung tissue sections showed that PrE-to-CBNPs caused lung

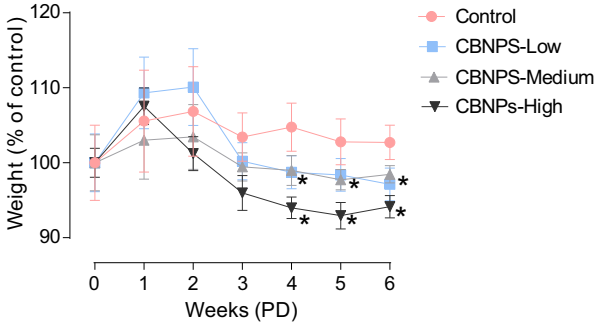

Fig. 2. Effect of PrE-to-CBNPs on weigh change.
Notes: The weight changes after CBNPs exposure. PD, post parturition; *p < 0.05.

injury (inclusive of interstitial thickening, hemorrhage and inflammatory cell influx) (Fig. 3A), and the degrees of lung injury were quantified (Fig. 3B). Strikingly, H&E stain results clearly showed that deposition of CBNPs in lung tissues in a dose-dependent manner (Fig. 3A). Our data indicated that PrE-to-CBNPs would cause lung damage, particularly in Medium- and High-dose CBNPs group. Intriguingly, we found that lung wet/dry weight ratio (an indicator for lung edema) was not significantly changed (Fig. S1). To investigate which type of inflammatory cells were infiltrated, we performed immunohistochemistry (IHC) stain with macrophage cell marker CD68 and neutrophil cell marker myeloperoxidase (MPO). Interestingly, infiltration of macrophage cell was observed (Fig. 4A), however the infiltration of neutrophil cell was negligible (Fig. S2). Consistently, we also found that PrE-to-CBNPs resulted in the pronounced elevation of cell count in BALF, which was a hallmark of inflammation in lung tissues (Fig. 4B). Meanwhile, we found that the mRNA expression of inflammatory cytokines IL-6, TNF-α and IL-1β increased in the PrE-to CBNPs group (Fig. 4C). In addition, we also found that oxidative stress markers heme oxygenase 1 (HO-1), nuclear factor erythroid 2–related factor 2 (Nrf-2) and C/EBP homologous protein (CHOP) [25,26] were elevated in response to pregnancy CBNPs exposure (Fig. 4D–E). Our results clearly indicated that PrE-to-CBNPs could cause persistent lung injury through inducing oxidative stress and inflammation.

3.3. Deposition of CBNPs in lysosomes induced lysosomal dysfunction

To investigate the underlying mechanisms of CBNPs-induced persistent dysfunction, we performed masson's trichrome stain. Interestingly, we failed to detect any collagen fibers in lung tissues (Fig. S3), indicating that CBNPs might not induce lung fibrosis. Transmission electron microscopy (TEM) results showed that CBNPs deposited in lysosomes in the pulmonary alveoli of dams (Fig. 5A). We also found that the lysosome marker, lysosomal associated membrane protein 1 (LAMP-1) was upregulated in a CBNPs dose-dependent manner (Fig. 5B–C), suggesting the amount of lysosomes was elevated in response to CBNPs exposure. Cathepsin D (CTSD) is a ubiquitously expressed lysosomal aspartyl protease involved in the normal degradation of proteins in lysosome. Our results showed that CTSD was down-regulated upon CBNPs treatment (Fig. 5D–E), indicating that dysfunction of lysosomes was induced by CBNPs exposure.

3.4. Pregnancy exposure to CBNPs caused autophagic dysfunction

Because lysosomes are the central hub of autophagy process, we suspected that lysosomal dysfunction would result in the dysfunction of autophagy. We found that the autophagosomes marker microtubule-associated proteins light chain 3 (LC3B)-II was elevated in a CBNPs dose-dependent manner (Fig. 6A–B), whereas no significant change of p62/SQSTM1 (substrate of autophagy) was observed (Fig. 6C–D). We further explored the possible regulation mechanism for the autophagy caused by PrE-to-CBNPs. Mammalian target of rapamycin (mTOR) is a key component that coordinately regulates the balance between growth and autophagy in response to cellular physiological conditions and environmental stress [27]. Activation of mTOR by nutrients and growth factors leads to inhibition of autophagy. Conversely, decreased mTOR leads to activation of autophagy through the phosphorylation of multiple autophagy-related proteins, such as ULK1, ATG13, AMBRA1, and ATG14L, which promote autophagy initiation and autophagosome nucleation [28]. Western blot results showed that profoundly decrease of p-mTOR (Ser2448) (Fig. 6E–F). Our results suggested that mTOR pathway might be involved in the dysfunction of autophagy caused by CBNPs exposure.

4. Discussion

Due to complex metabolic changes and to the higher susceptibility

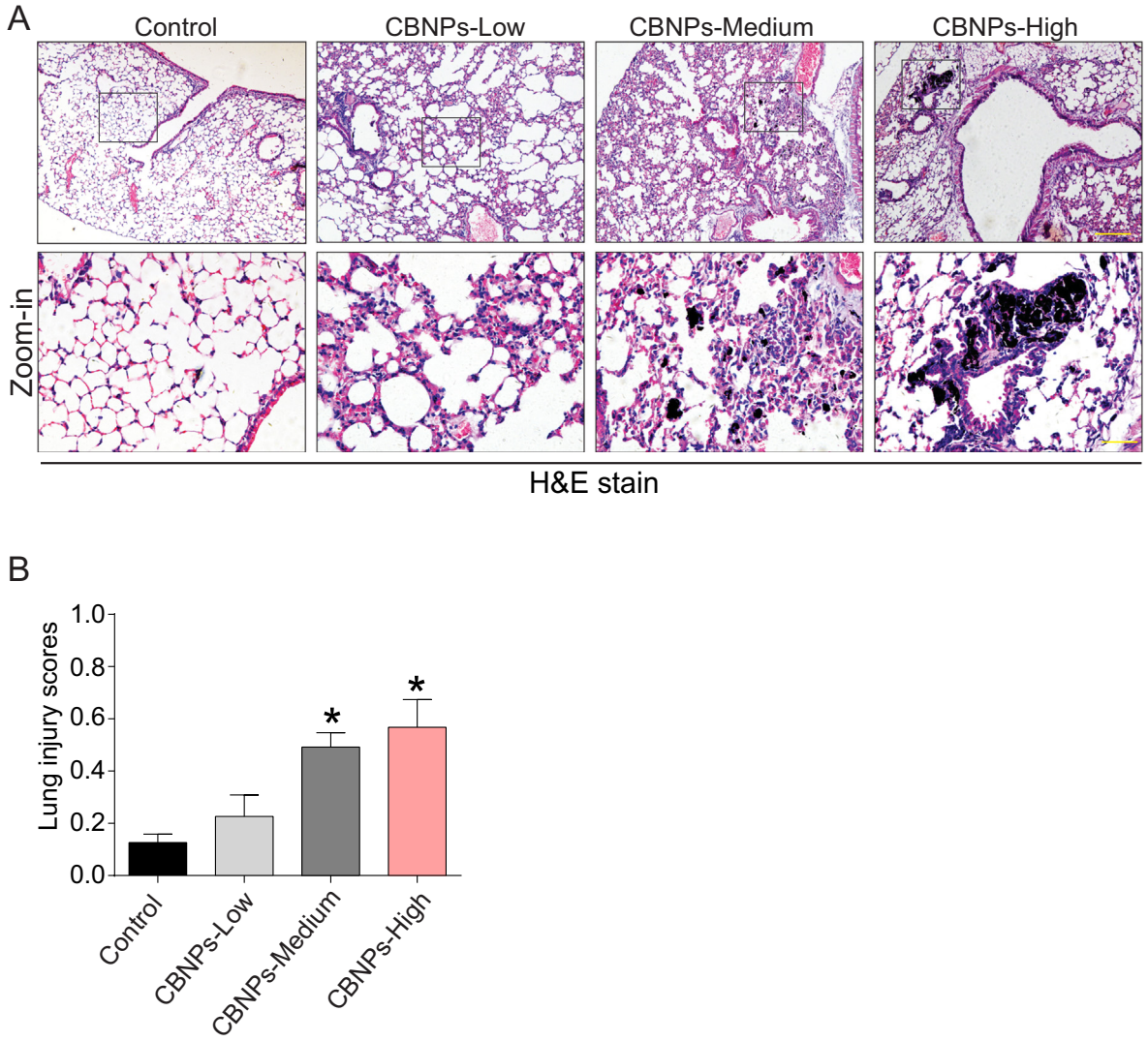

Fig. 3. PrE-to-CBNPs resulted in lung damage.
Notes: (A) Histopathological changes at 49 days after parturition were determined by H&E stain. The upper panel is 100× magnification (scale bar = 200 μm) and the lower panel is 400× magnification (scale bar = 50 μm). (B) The lung injury scores were quantified. *$p < 0.05$.

of the developing tissues to environmental stimulus, pregnancy exposure to nanomaterials attracts great interests. The relevance of investigating the effect of maternal exposure to nanomaterials has recently emerged [29]. Accumulating evidence supports the notion that the fetus may be more sensitive to chemical exposures than the adult organism, however whether maternal exposure to nanomaterials may constitute a hazard to pregnant female themselves remains to be clarified [30]. In particular, long-term effects on the dams after PrE-to-CBNPs are largely unknown. We report here, which is distinct from previous studies, pregnancy exposure (GD9-GD18) to CBNPs would result in persistent lung injury even 49 days after parturition, and this long-term pulmonary toxic effect of CBNPs in pregnant mice is dose dependent.

In this study, we treated the pregnant mice with CBNPs *via* intranasal exposure for 10 days, and observed the prolonged effects at 49 days after parturition. We used this experimental design based on the following two concerns. Firstly, previous studies have been revealed that > 50% of inhaled nanoparticles (diameter < 20 nm) can accumulate in alveolar tissue [31] and can gradually distribute in the whole lung by physical diffusion, lymphatic transfer or phagocytosis [32]. More importantly, the CBNPs is difficult to discharge through metabolic pathways, therefore may exist in the body for a relative long time [33]. Secondly, given that CBNPs cannot be easily eliminated, it is plausible that the accumulation of inhaled CBNPs would result in delayed or cumulative toxicity in lung tissues. Moreover, the long-term persistent or delayed toxicity usually observed longer than one month. Therefore, we chose the observation endpoint at 49 days after parturition.

The current study suggests that lysosomes are likely the target of CBNPs. Lysosomes are the central hub of autophagic process, because the cargo (including aberrant protein, organelle or foreign matter) in the autophagosomes or endosomes should be digested in lysosomes. Our study found that although the number of lysosomes increased (the increase of LAMP-1 expression), however the expression level of CTSD dramatically decreased. CTSD is a major lysosomal endopeptidase, which is critical in the degradation of long-lived proteins [34]. Genetic and clinical studies have shown that the homozygous deficiency or heterozygous missense mutations of CTSD are associated in multiply diseases [35,36]. We infer that the biogenesis of lysosomes was activated to digest exogenous CBNPs, however undissolved CBNPs deposited in the lysosomes to result in the dysfunction of lysosomes. Consequently, the elevated expression of LC3B-II was observed. A previous study claimed that male C57BL6 mice exposure to 20 μg CBNPs would resulted in the elevation of LC3B but not significant change in LAMP-2 expression and inflammation 7 days after exposure

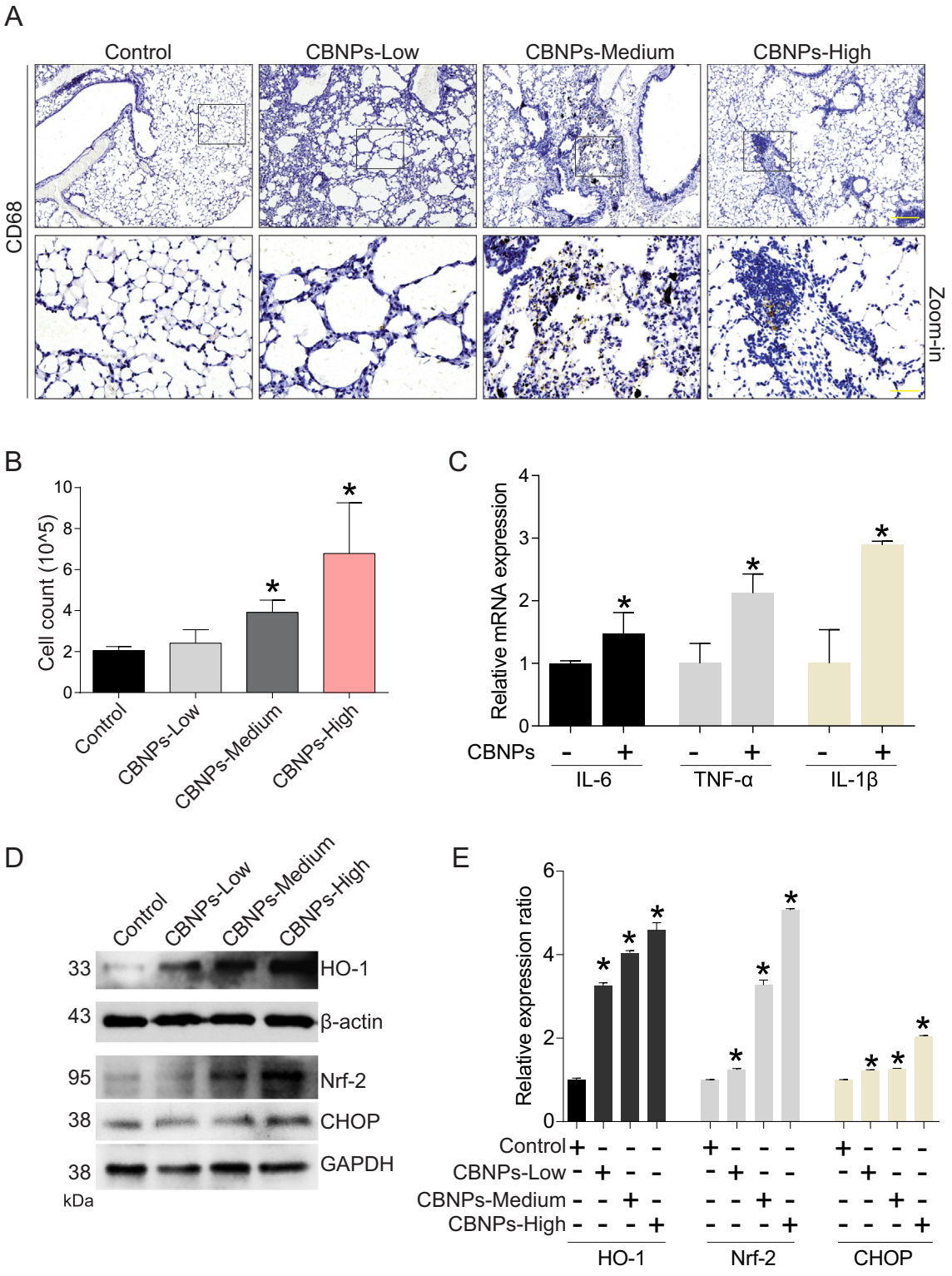

Fig. 4. PrE-to-CBNPs caused inflammation and oxidative stress in lung of dams.
Notes: (A) Infiltration of macrophage cell in the lung at 49 days after parturition was determined by immunohistochemistry stain. CD68 was used as macrophage marker. The upper panel is 100× magnification (scale bar = 200 μm) and the lower panel is 400× magnification (scale bar = 50 μm). (B) The cell counts in the bronchoalveolar lavage fluid were counted. *$p < 0.05$. (C) The mRNA expression levels of IL-6, TNF-α and IL-1β were determined by QPCR assay. (D) Western-blot experiment was performed to detect the expression level of HO-1, Nrf-2 and CHOP in the mouse lung tissue; β-actin or GAPDH was served as loading control. (E) The relative expression levels of HO-1, Nrf-2 and CHOP were presented. *$p < 0.05$.

[37]. This disparity might be due to the different mice, dosage of CBNPs and the observation time. The profile of toxicity induced by CBNPs seems distinct from copper oxide nanoparticles (CuONPs) we previously studied. We found that CuONPs could deposited in lysosomes to enhance their dissolution to release copper ions [38], which could damage mitochondria and result in the accumulation of

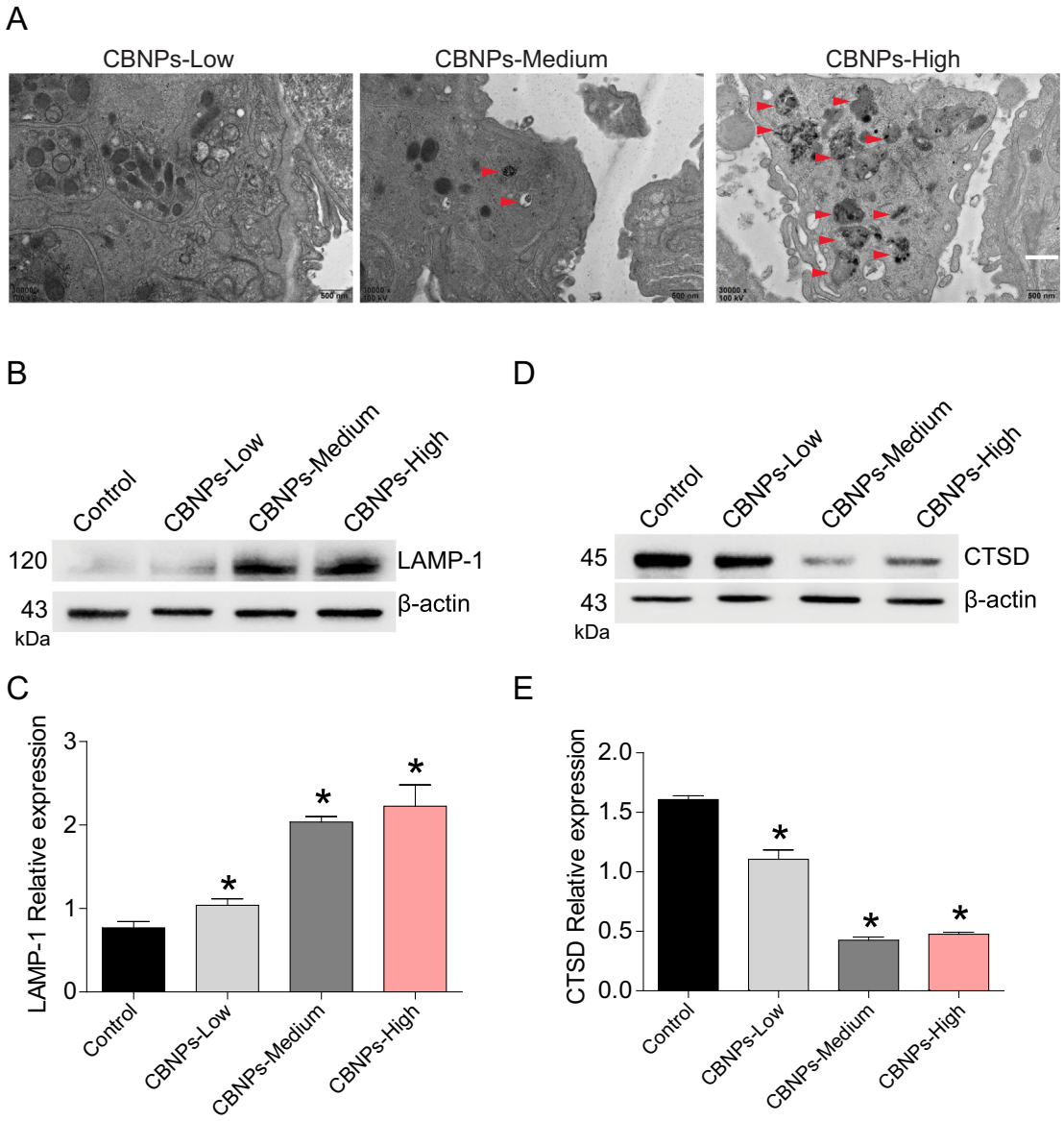

Fig. 5. CBNPs deposited in lysosome and induced lysosomal dysfunction.
Notes: (A) TEM images showed that the accumulation of lysosomes upon CBNPs exposure in the pulmonary alveoli. The red arrows indicated the deposition of CBNPs in the lysosomes. Scale bar = 500 μm. (B–C) The expression level of LAMP-1 in mouse lung tissue was determined by western-blot and was quantified against loading control, β-actin. (D–E) The expression level of CTSD in mouse lung tissue was determined by western-blot and was quantified against loading control, β-actin. *$p < 0.05$. (For interpretation of the references to colour in this figure legend, the reader is referred to the web version of this article.)

superoxide anions and ultimately the cell death in endothelial cell [39]. However, the pregnancy exposure experiments are not feasible to perform *in vitro*. Hence, we just concluded that lysosomal dysfunction is probably associated with lung injury in dams who pregnancy exposure to CBNPs. The crosstalk between lysosomal and mitochondrial dysfunction caused by pregnancy CBNPs exposure needs further investigations.

Meanwhile, we found several unique characteristics of this PrE-to-CBNPs model. Firstly, the results of masson's trichrome stain suggested that negligible fibrosis induced by CBNPs. Secondly, PrE-to-CBNPs resulted in the infiltration of macrophage while not neutrophil, which was distinct from endotoxin-induced lung injury. In fact, beyond the lysosomal dysfunction caused by CBNPs reported herein, more biological effects of CBNPs had been explored recently. For example, nanoparticulate carbon black in cigarette smoke could induce DNA cleavage and Th17-mediated emphysema [40]; Exposure of macrophages (both a macrophage cell line and primary human alveolar macrophages) to carbon black nanoparticles induces pyroptosis, an inflammasome-dependent form of cell death, as defined by cleavage of caspase 1 to its active form and downstream IL-1β release [7]; CBNPs was reported to generate vasomotor dysfunction in artery segments [41]. Therefore, the molecular mechanisms for CBNPs-induced toxicity remain to be further clarified since the biological effects of CBNPs are diverse.

Overall, we found that PrE-to-CBNPs could cause persistent lung injury, which is distinct form endotoxin- or bleomycin-induced lung injury. The deposition of CBNPs in lysosomes in the lung tissues of dams might be responsible for the lysosomal dysfunction, which might be associated with the long-term lung injury caused by PrE-to-CBNPs in dams.

Acknowledgements

This research was financially supported by National Science Foundation of China (81602820, 81703187 and 81300057),

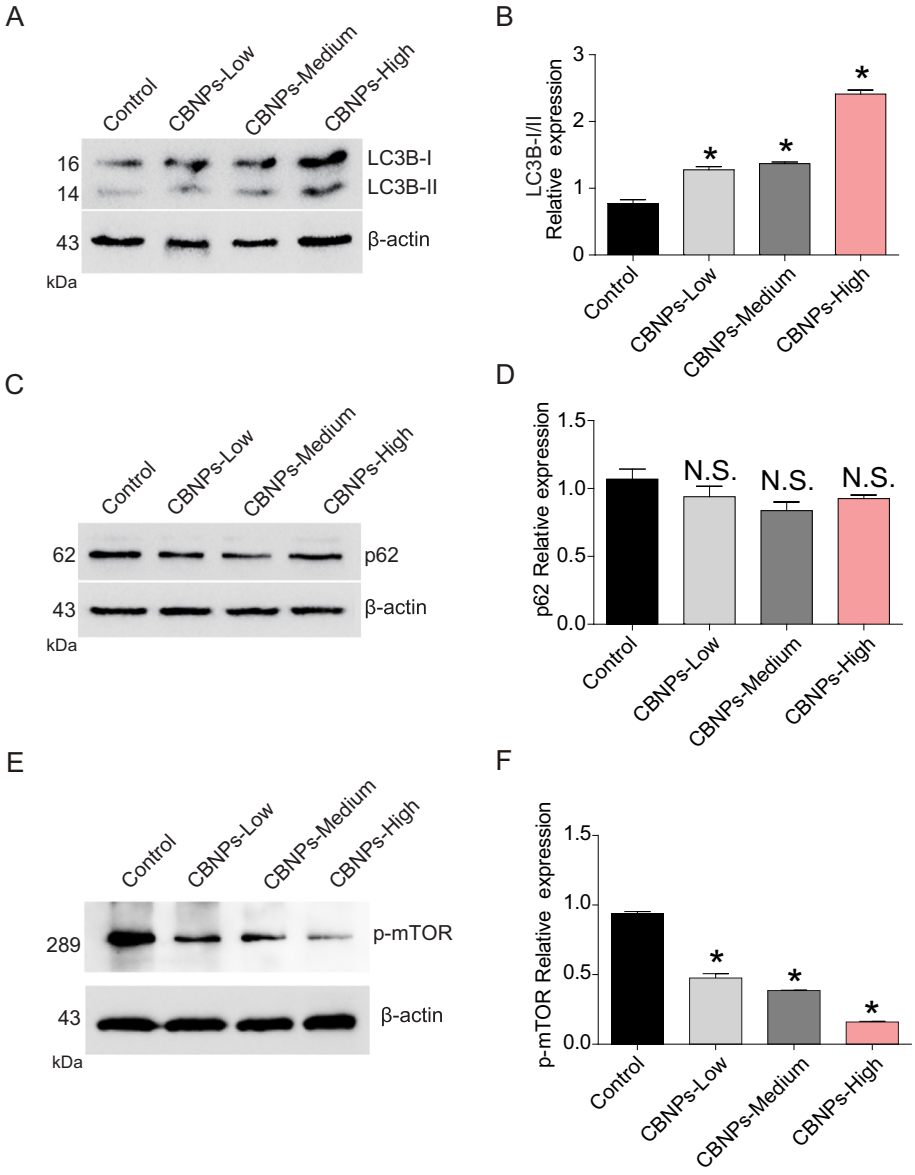

Fig. 6. CBNPs exposure suppressed mTOR and led to autophagy induction.
Notes: (A–B) The expression level of LC3B in mouse lung tissue was determined by western-blot and was quantified against loading control β-actin. (C–D) The expression level of p62 in mouse lung tissue was determined by western-blot and was quantified against loading control, β-actin. (E–F) The expression level of p-mTOR in mouse lung tissue was determined by western-blot and was quantified against loading control, β-actin. *$p < 0.05$. N.S., not significant.

Foundation and Frontier Research Program of Chongqing Science and Technology Commission (cstc2017jcyjAX0162, cstc2016jcyjA0223 and cstc2016jcyjA0435), Science and Technology Research Program of Chongqing Municipal Education Commission (KJQN201800434), China Postdoctoral Science Foundation funded project (2017M612925 and 2018T110951), Postdoctoral Research Project of Chongqing Municipality (XM2017003) and the Commission of Science and Technology of Yuzhong district of Chongqing (20160101).

Declaration of competing interest

The authors declare no conflict of interest.

Appendix A. Supplementary data

Supplementary data to this article can be found online at https://doi.org/10.1016/j.lfs.2019.116741.

References

[1] P. Harber, H. Muranko, S. Solis, A. Torossian, B. Merz, Effect of carbon black exposure on respiratory function and symptoms, J. Occup. Environ. Med. 45 (2003) 144–155.
[2] N.L. Mills, K. Donaldson, P.W. Hadoke, N.A. Boon, W. MacNee, F.R. Cassee, et al., Adverse cardiovascular effects of air pollution, Nat. Clin. Pract. Cardiovasc. Med. 6 (2009) 36–44.
[3] L.K. Vesterdal, J.K. Folkmann, N.R. Jacobsen, M. Sheykhzade, H. Wallin, S. Loft, et al., Pulmonary exposure to carbon black nanoparticles and vascular effects, Part. Fibre Toxicol. 7 (2010) 33.
[4] J.A. Bourdon, A.T. Saber, N.R. Jacobsen, K.A. Jensen, A.M. Madsen, J.S. Lamson, et al., Carbon black nanoparticle instillation induces sustained inflammation and genotoxicity in mouse lung and liver, Part. Fibre Toxicol. 9 (2012) 5.
[5] D. Saputra, J.H. Yoon, H. Park, Y. Heo, H. Yang, E.J. Lee, et al., Inhalation of carbon black nanoparticles aggravates pulmonary inflammation in mice, Toxicol. Res. 30 (2014) 83–90.
[6] K. Lindner, M. Strobele, S. Schlick, S. Webering, A. Jenckel, J. Kopf, et al., Biological effects of carbon black nanoparticles are changed by surface coating with polycyclic aromatic hydrocarbons, Part. Fibre Toxicol. 14 (2017) 8.
[7] A.C. Reisetter, L.V. Stebounova, J. Baltrusaitis, L. Powers, A. Gupta, V.H. Grassian, et al., Induction of inflammasome-dependent pyroptosis by carbon black nanoparticles, J. Biol. Chem. 286 (2011) 21844–21852.

[8] I. Chaudhuri, C. Fruijtier-Polloth, Y. Ngiewih, L. Levy, Evaluating the evidence on genotoxicity and reproductive toxicity of carbon black: a critical review, Crit. Rev. Toxicol. 48 (2018) 143–169.
[9] Y.S. El-Sayed, R. Shimizu, A. Onoda, K. Takeda, M. Umezawa, Carbon black nanoparticle exposure during middle and late fetal development induces immune activation in male offspring mice, Toxicology 327 (2015) 53–61.
[10] P. Jackson, K.S. Hougaard, U. Vogel, D. Wu, L. Casavant, A. Williams, et al., Exposure of pregnant mice to carbon black by intratracheal instillation: toxicogenomic effects in dams and offspring, Mutat. Res. 745 (2012) 73–83.
[11] Y. Zhang, B. Tu, X. Jiang, G. Xu, X. Liu, Q. Tang, et al., Exposure to carbon black nanoparticles during pregnancy persistently damages the cerebrovascular function in female mice, Toxicology 422 (2019) 44–52.
[12] J.P. Luzio, P.R. Pryor, N.A. Bright, Lysosomes: fusion and function, Nat. Rev. Mol. Cell Biol. 8 (2007) 622–632.
[13] H. Appelqvist, P. Waster, K. Kagedal, K. Ollinger, The lysosome: from waste bag to potential therapeutic target, J. Mol. Cell Biol. 5 (2013) 214–226.
[14] D.R. Green, L. Galluzzi, G. Kroemer, Mitochondria and the autophagy-inflammation-cell death axis in organismal aging, Science 333 (2011) 1109–1112.
[15] D. Glick, S. Barth, K.F. Macleod, Autophagy: cellular and molecular mechanisms, J. Pathol. 221 (2010) 3–12.
[16] L. Yu, Y. Chen, S.A. Tooze, Autophagy pathway: cellular and molecular mechanisms, Autophagy 14 (2018) 207–215.
[17] S.T. Stern, P.P. Adiseshaiah, R.M. Crist, Autophagy and lysosomal dysfunction as emerging mechanisms of nanomaterial toxicity, Part. Fibre Toxicol. 9 (2012) 20.
[18] P. Pocar, N. Fiandanese, A. Berrini, C. Secchi, V. Borromeo, Maternal exposure to di (2-ethylhexyl)phthalate (DEHP) promotes the transgenerational inheritance of adult-onset reproductive dysfunctions through the female germline in mice, Toxicol. Appl. Pharmacol. 322 (2017) 113–121.
[19] S. Akira, S. Uematsu, O. Takeuchi, Pathogen recognition and innate immunity, Cell 124 (2006) 783–801.
[20] P. Jackson, K.S. Hougaard, A.M. Boisen, N.R. Jacobsen, K.A. Jensen, P. Moller, et al., Pulmonary exposure to carbon black by inhalation or instillation in pregnant mice: effects on liver DNA strand breaks in dams and offspring, Nanotoxicology 6 (2012) 486–500.
[21] X. Jiang, Q. Tang, J. Zhang, H. Wang, L. Bai, P. Meng, et al., Autophagy-dependent release of zinc ions is critical for acute lung injury triggered by zinc oxide nanoparticles, Nanotoxicology 12 (2018) 1068–1091.
[22] G. Matute-Bello, G. Downey, B.B. Moore, S.D. Groshong, M.A. Matthay, A.S. Slutsky, et al., An official American Thoracic Society workshop report: features and measurements of experimental acute lung injury in animals, Am. J. Respir. Cell Mol. Biol. 44 (2011) 725–738.
[23] L. Zhang, S. Cheng, X. Jiang, J. Zhang, P. Meng, Q. Tang, et al., Pregnancy exposure to carbon black nanoparticles exacerbates bleomycin-induced lung fibrosis in offspring via disrupting LKB1-AMPK-ULK1 axis-mediated autophagy, Toxicology 425 (2019) 152244.
[24] J. Zhang, X. Qin, B. Wang, G. Xu, Z. Qin, J. Wang, et al., Zinc oxide nanoparticles harness autophagy to induce cell death in lung epithelial cells, Cell Death Dis. 8 (2017) e2954.
[25] J.A. Araujo, M. Zhang, F. Yin, Heme oxygenase-1, oxidation, inflammation, and atherosclerosis, Front. Pharmacol. 3 (2012) 119.
[26] Q. Ma, Role of nrf2 in oxidative stress and toxicity, Annu. Rev. Pharmacol. Toxicol. 53 (2013) 401–426.
[27] C.H. Jung, S.H. Ro, J. Cao, N.M. Otto, D.H. Kim, mTOR regulation of autophagy, FEBS Lett. 584 (2010) 1287–1295.
[28] Y.C. Kim, K.L. Guan, mTOR: a pharmacologic target for autophagy regulation, J. Clin. Invest. 125 (2015) 25–32.
[29] L. Campagnolo, M. Massimiani, L. Vecchione, D. Piccirilli, N. Toschi, A. Magrini, et al., Silver nanoparticles inhaled during pregnancy reach and affect the placenta and the foetus, Nanotoxicology 11 (2017) 687–698.
[30] K.S. Hougaard, L. Campagnolo, P. Chavatte-Palmer, A. Tarrade, D. Rousseau-Ralliard, S. Valentino, et al., A perspective on the developmental toxicity of inhaled nanoparticles, Reprod. Toxicol. 56 (2015) 118–140.
[31] G. Oberdorster, E. Oberdorster, J. Oberdorster, Nanotoxicology: an emerging discipline evolving from studies of ultrafine particles, Environ. Health Perspect. 113 (2005) 823–839.
[32] L.C. Renwick, D. Brown, A. Clouter, K. Donaldson, Increased inflammation and altered macrophage chemotactic responses caused by two ultrafine particle types, Occup. Environ. Med. 61 (2004) 442–447.
[33] W.I. Hagens, A.G. Oomen, W.H. de Jong, F.R. Cassee, A.J. Sips, What do we (need to) know about the kinetic properties of nanoparticles in the body? Regul. Toxicol. Pharmacol. 49 (2007) 217–229.
[34] R.T. Dean, Lysosomes and protein degradation, Acta Biol. Med. Ger. 36 (1977) 1815–1820.
[35] E. Siintola, S. Partanen, P. Stromme, A. Haapanen, M. Haltia, J. Maehlen, et al., Cathepsin D deficiency underlies congenital human neuronal ceroid-lipofuscinosis, Brain 129 (2006) 1438–1445.
[36] E.J. Bae, N.Y. Yang, C. Lee, S. Kim, H.J. Lee, S.J. Lee, Haploinsufficiency of cathepsin D leads to lysosomal dysfunction and promotes cell-to-cell transmission of alpha-synuclein aggregates, Cell Death Dis. 6 (2015) e1901.
[37] H. Kong, K. Xia, L. Pan, J. Zhang, Y. Luo, Y. Zhang, et al., Autophagy and lysosomal dysfunction: a new insight into mechanism of synergistic pulmonary toxicity of carbon black-metal ions co-exposure, Carbon 111 (2017) 322–333.
[38] J. Zhang, Z. Zou, B. Wang, G. Xu, Q. Wu, Y. Zhang, et al., Lysosomal deposition of copper oxide nanoparticles triggers HUVEC cells death, Biomaterials 161 (2018) 228–239.
[39] J. Zhang, B. Wang, H. Wang, H. He, Q. Wu, X. Qin, et al., Disruption of the superoxide anions-mitophagy regulation axis mediates copper oxide nanoparticles-induced vascular endothelial cell death, Free Radic. Biol. Med. 129 (2018) 268–278.
[40] R. You, W. Lu, M. Shan, J.M. Berlin, E.L. Samuel, D.C. Marcano, et al., Nanoparticulate carbon black in cigarette smoke induces DNA cleavage and Th17-mediated emphysema, eLife 4 (2015) e09623.
[41] L.K. Vesterdal, L. Mikkelsen, J.K. Folkmann, M. Sheykhzade, Y. Cao, M. Roursgaard, et al., Carbon black nanoparticles and vascular dysfunction in cultured endothelial cells and artery segments, Toxicol. Lett. 214 (2012) 19–26.